# Seismic inversion using a geostatistical, petrophysical, and acoustic model

MIGUEL BOSCH, Universidad Central de Venezuela CORAL CAMPOS, Suelopetrol ELSA FERNÁNDEZ, Info-Gestión Consultores

Interpretation of seismic data for structure and stratigraphy is commonly based on the geological knowledge of the area and the correlation of seismic reflections with well-log data. However, the relation between the seismic image and the well-log data is not straightforward, being often obscured by the wave-propagation phenomenon. Part of the problem is that reflectivities do not measure the interval properties but result from the property contrasts of consecutive strata. Seismic inversion provides insight into the interpretation process, transforming reflection amplitudes into physically meaningful variations in interval properties, which can be directly related to the well-log data after appropriate scale considerations.

In the present work, we combine well-log and seismic reflection data for delineation of the major stratification in a producing oil reservoir in Ecuador. Production in this field is obtained from sandstone strata; the stratification involves several sequences of shale, carbonates, and sands. Based on the relationship between the acoustic impedance and the total porosity, we jointly estimate both properties in the seismic inversion. In addition, by constraining the seismic inversion with well-log data, we improve the vertical resolution of the estimated fields beyond normal seismic resolution, and the correlation between the estimated fields and the well-log information.

We analyze the seismic data under the acoustic approximation. Further extension of this type of integrated analysis that considers elastic modeling of prestack or partial-stacked data is envisaged in this area in future, with the acquisition of new seismic data with longer offsets.

## Petrophysical relationships

Figure 1 shows a crossplot of the acoustic impedance against the total porosity as calculated from the well-log data and plotted at well-log resolution for a typical well in this area. The colors categorize the major lithotypes in the stratigraphic sequence. The variation of the acoustic impedance is largely anticorrelated with the total porosity, as expected from common petrophysical models. Also, it is evident that in this area high total porosity (> 0.2) or low acoustic impedance (< 9  $\times$   $10^6 \ kg/m^2$  s) are good indicators for shale, whereas the high-impedance or low-porosity rocks mostly correspond to sands and carbonates.

To integrate the seismic and well-log data, we develop a two-scale model: The acoustic impedance is parameterized at two different time intervals related by an appropriate scale transform. This transform determines the low-resolution level of the model as a function of the high-resolution level, i.e., the equivalent properties of a thick layer as a function

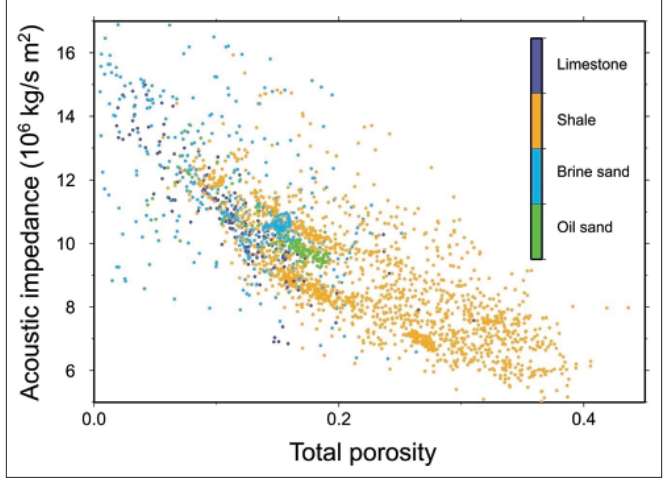


Figure 1. Crossplot of well-log-derived acoustic impedance against total porosity at the original sampling interval for one well in the area. Colors show classification of the samples according to major lithological groups.

of the properties of the finer constitutive layers. We set the low-resolution-model scale commensurate with the seismic resolution, which depends on the frequency content of the reflected wavelet. It is used for reflectivity calculation and fixed to a 4-ms sampling interval for the results shown in this work. The objective function, as given by Equation 1, is formulated at the high-resolution level. For computational and interpretational reasons, we set the high-resolution scale at an intermediate point between the original well-log resolution and the seismic resolution. In this work, we use a 1-ms sampling interval for the model's high-resolution scale, with an improvement of four times in the resolution of the vertical model.

Figure 2a shows a crossplot of the acoustic impedance and total porosity upscaled to a 1-ms time-sampling interval for the well-log data in Figure 1. The deviations of the samples are smaller, and the dependency trend is clearer in the rescaled crossplot. Using a petrophysical model that combines the Wyllie and Wood relationships, we parameterize and calibrate to the experimental rescaled data a statistical model for the dependency between the impedance and porosity. Figure 2a also shows the calibrated petrophysical transform fitting the experimental impedance versus porosity data obtained by regression, and the gray band that indicates the deviations of the experimental data from the model (plus or minus one standard deviation). For building up the statistical porosityimpedance model, we also characterize the time covariances for the porosity and for the acoustic impedance deviations from the calibrated petrophysical transform.

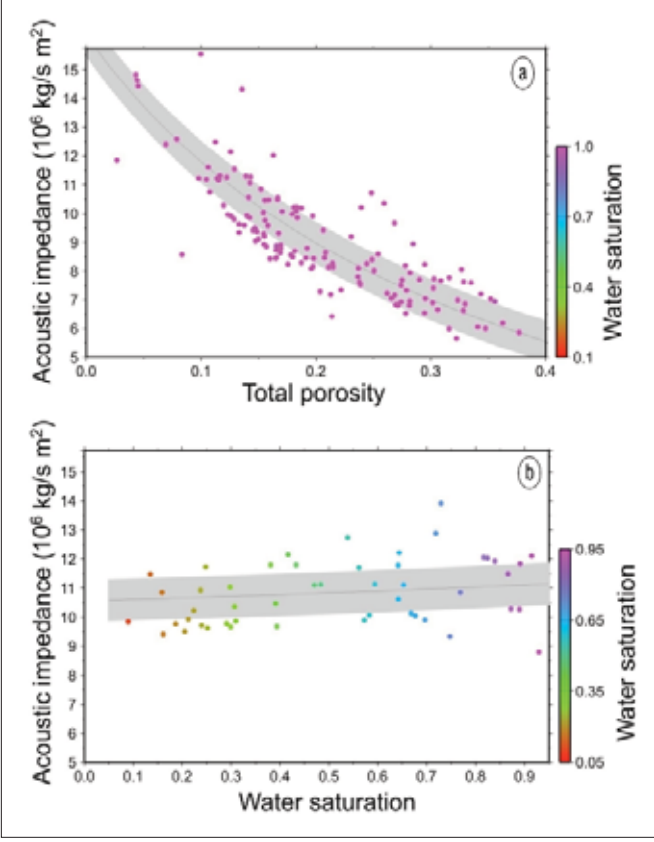


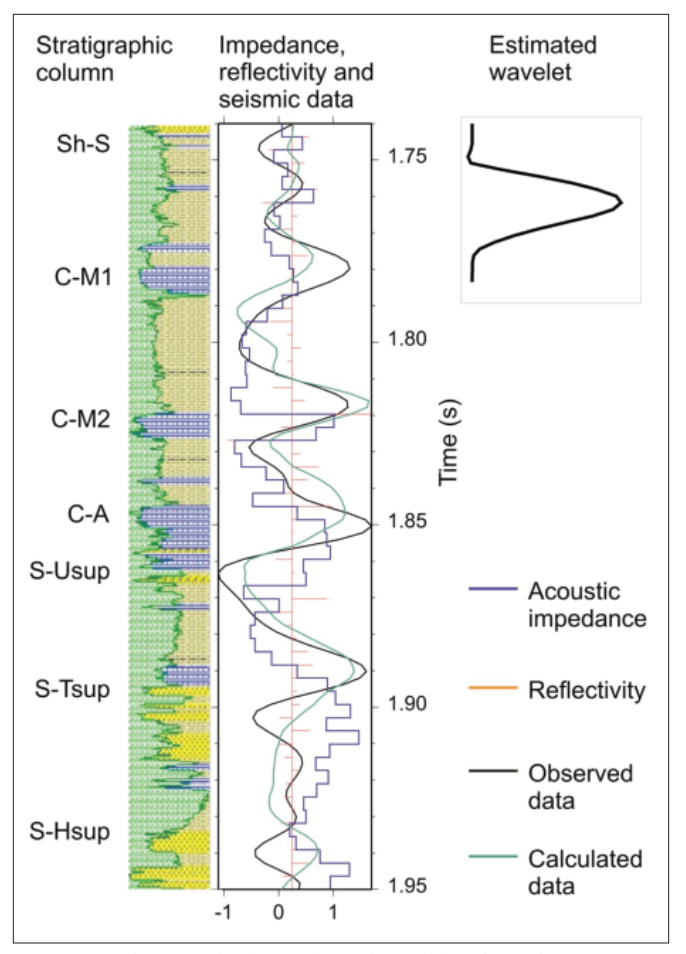
Figure 2. Crossplots of well-log properties rescaled at 1-ms reflection time interval for the well in Figure 1: acoustic impedance against (a) total porosity and (b) water saturation. Colors indicate water saturation in the two plots. The black line shows the petrophysical transform calibrated to the well-log data, and the gray band indicates plus and minus one standard acoustic impedance deviation from the transform used in the petrophysical statistical model.

Figure 2b shows the relation between the acoustic impedance and water saturation for a porosity range that encompasses the oil-bearing sands. The plot clearly shows the expected effect of oil in reducing the acoustic impedance of the rock. However, the small size of the fluid effect compared to the corresponding effect of the total porosity (shown in Figure 2a) means fluid discrimination is beyond the resolution of the acoustic inversion in this work.

#### Seismic modeling

We modeled the time-migrated data by calculating reflectivities under the acoustic formulation (normal incidence) and convolving the reflectivity series with a source wavelet (Figure 3). The source wavelet is estimated by a least-squares fitting of the observed and calculated seismic data; no phase assumptions were used. A good fit between the observed and calculated traces shows that, although we are modeling in the acoustic approximation of reflectivity, the observed seismic amplitudes are satisfactorily explained by the well-log data.

Figure 3 also shows the stratigraphic sequence corresponding to this well, interpreted from well-log data. The major positive reflections result from the contact of a thick



**Figure 3.** The central column shows the well-log-derived acoustic impedance, the corresponding reflectivities, the observed seismic amplitudes, and the amplitudes calculated from the well-log reflectivity. The estimated wavelet is shown at the third column. Text at the left corresponds to strata: S = s and S = s carbonates, and S = s shale.

shale stratum with a consecutive carbonate stratum. Sandstone strata are commonly beneath the limestone. The acoustic behavior of carbonate and sand are similar in this area and difficult to discriminate, as previously shown from the well-log data. On the other hand, low acoustic impedance is clearly associated with thick shale strata.

#### Inverse problem formulation

Our inversion method is based on minimizing a combined objective function, S, that includes a seismic likelihood term, a petrophysical likelihood term, and a geostatistical prior term,

$$S = S_{seis} + S_{petro} + S_{geos}$$
 (1)

For each CDP, the acoustic impedance and total porosity are defined in a sequence of layers of uniform traveltime thickness. The objective function is defined independently for each joint porosity and impedance model at each CDP. In the above expression, the seismic likelihood term, S<sub>scis</sub>, measures the CDP model deviations between the observed and calcu-

lated seismic data. The petrophysical likelihood term, S petro, measures the CDP model deviations between the acoustic impedance model and the petrophysical transform of the porosity, i.e., the theoretical impedances calculated from the porosity model with the petrophysical function calibrated in a preceding section. The geostatistical term, S geos, measures the deviations of the CDP model porosity and impedance from the prior fields, which play the role of background model for the seismic and petrophysical inversion. In the case of well-log conditioning, the prior porosity and impedance fields are obtained from geostatistical interpolation of the well-log data (cokriging) at the high-resolution-model scale. The joint inverse formulation combines the information across non-linearly related parameters, improving the exactitude of the estimated reservoir properties.

The three terms in Equation 1 are quadratic and include: the data covariance associated to the observation and calculation uncertainties; the property covariance across different time layers of the same CDP model; and the spatial covariance between the well-log data and the CDP properties. For the results in the next sections, we use a data standard deviation of 2% of the maximum range of the trace amplitude for the seismic likelihood term. More detail on this method can be found in Bosch et al. (2009).

## Seismic petrophysical inversion

If no conditioning to well-log data is considered, the geostatistical term reduces to a prior information term measuring deviations of the impedance and porosity fields from the prior background model. We used a uniform prior model for the acoustic impedance and the total porosity, which corresponded to the mean values of the well logs at the inversion window. In this case, the petrophysical objective function term still enforces the petrophysical model that relates porosity and impedance for joint estimation of the two properties. This formulation can be named "petrophysical seismic inversion" as it integrates the seismic and petrophysical steps of inference.

We illustrate this inversion approach with a seismic line in the area. Figure 4 shows the observed seismic data calculated from the estimated property model obtained with the inversion, and a well. This well will be useful when comparing the inversion results with the well-log-derived properties for the petrophysical seismic inversion with no well conditioning.

Figure 5 shows the estimated acoustic impedance and total porosity for the petrophysical seismic inversion. No spatial conditioning to the well-log data is used in this case. The corresponding well-log-derived acoustic impedance and total porosity, upscaled to 1-ms sampling, are superposed. The figure shows that the inversion adequately maps major stratification in the reservoir in the acoustic-impedance and total-porosity fields, and agree at the seismic resolution scale with the well-log-derived properties. Resolution of the estimated fields corresponds to the seismic frequency content as expected from a seismic inversion. Thin strata, like sand S-M2 for instance, are not present in the estimated section. Also, major strata delineated in the inversion results do not show their particular

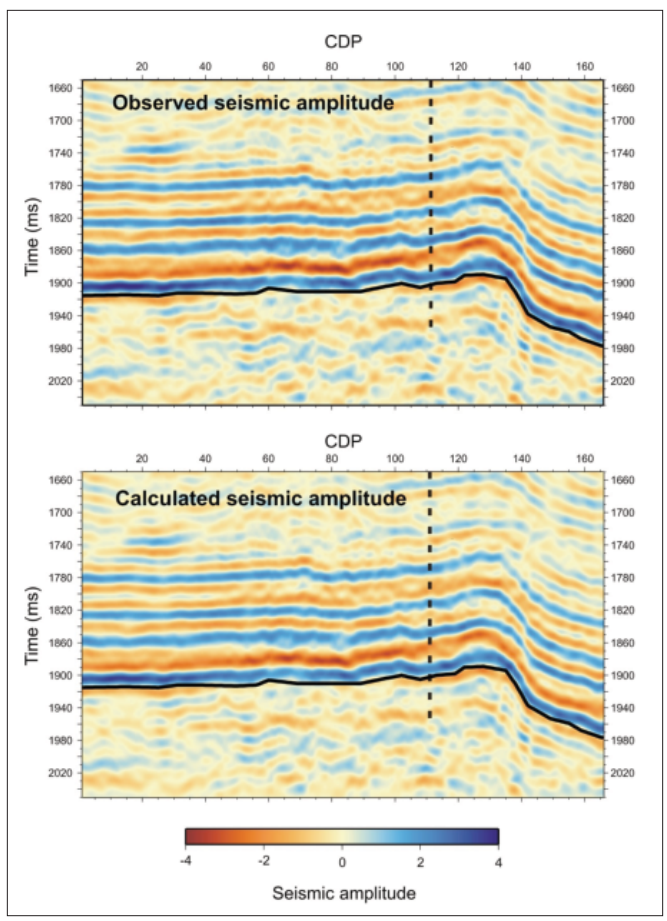


Figure 4. Observed stacked and time-migrated data for one line and the corresponding data calculated from the acoustic impedance obtained from the inversion and shown in Figure 5. The solid black line shows a polygon picked to follow a reference reflector on the seismic section. The dashed line indicates a well.

inner stratified structure, which is evident in the superposed well logs.

#### Seismic geostatistical and petrophysical inversion

In this approach, we condition the seismic inversion to the well-log data using a geostatistical model. The covariance function used in the inversion is characterized in the time direction from the actual rescaled well-log data. To guide the lateral covariance between the model property and welllog-derived property, the covariance function follows the geometry of a major horizon which is picked, in this case, from a continuous event in the seismic section. In the lateral directions, we use a Gaussian covariance model with large range considering the continuity that the stratification shows in the area. Figure 4 shows the reference horizon and the corresponding picked polygon used to mark appropriate time shifts for the lateral correlation between model and well-log properties. As the seismic inversion considers the spatial correlation with additional data (well logs) for the estimation of the impedance and porosity, this procedure can be named geostatistical and petrophysical seismic inversion.

Well-log-derived properties have higher spatial resolution along the well path than the inverted seismic proper-

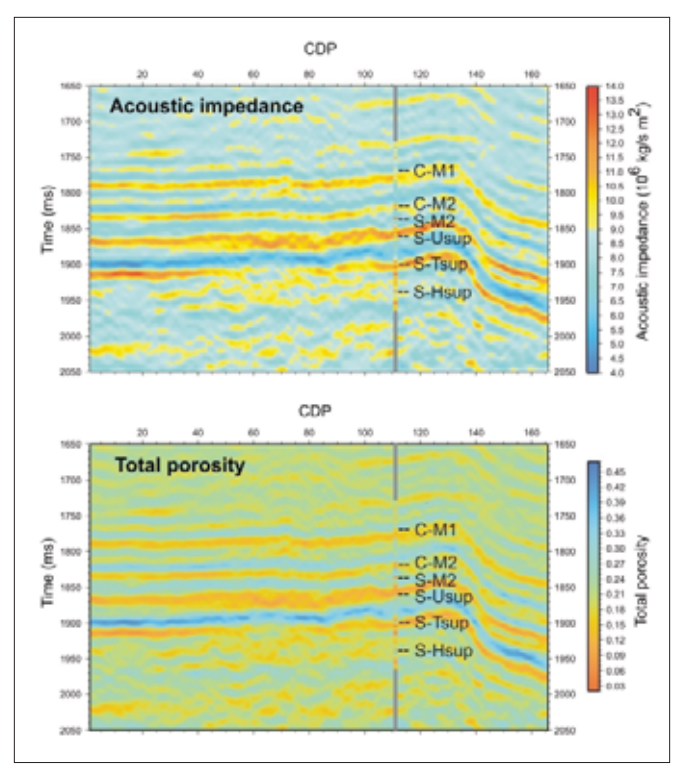


Figure 5. Acoustic-impedance and total-porosity sections resulting from the petrophysical inversion of the data in Figure 4 with no well-log conditioning. The acoustic impedance and total porosity calculated from the well-log data are superposed.

ties, and they often are considered as hard data (exact data). However, the exactitude and precision of the well-log-derived properties are subject to different uncertainty sources such as the tool calibration, effect of mud, wall geometry, and several corrections that are applied to the collected data. Hence, considering the well-log data as exact may bias the combined estimation problem. In our method, we calculate the well-log and seismic property covariance, including a correlation factor between the two types of properties, to account for the uncertainty of the well-log data. This is the maximum correlation that applies at the same spatial location of the well and model; for points away from the well, this correlation decreases according to the covariance function.

Figures 6b and 6c show results for the acoustic impedance obtained with 0.5 and 0.7 well log-to-model correlation and the geostatistical covariance model already described. Figure 6a shows the acoustic impedance model estimated with no correlation to the well-log data, as obtained in the previous section, for comparison with the inversion results spatially conditioned to the well-log data. The well-log-derived acoustic impedance is superposed. The estimated acoustic impedance obtained with the geostatistical and petrophysical seismic inversions agrees with the major stratification estimated without well conditioning. However, one relevant feature is the improved vertical resolution of the estimated property fields, which is inherited from the conditioning well-log information via the lateral covariance in the statistical model. In Figures 6b and 6c, sand strata S-M2, for instance, is present,

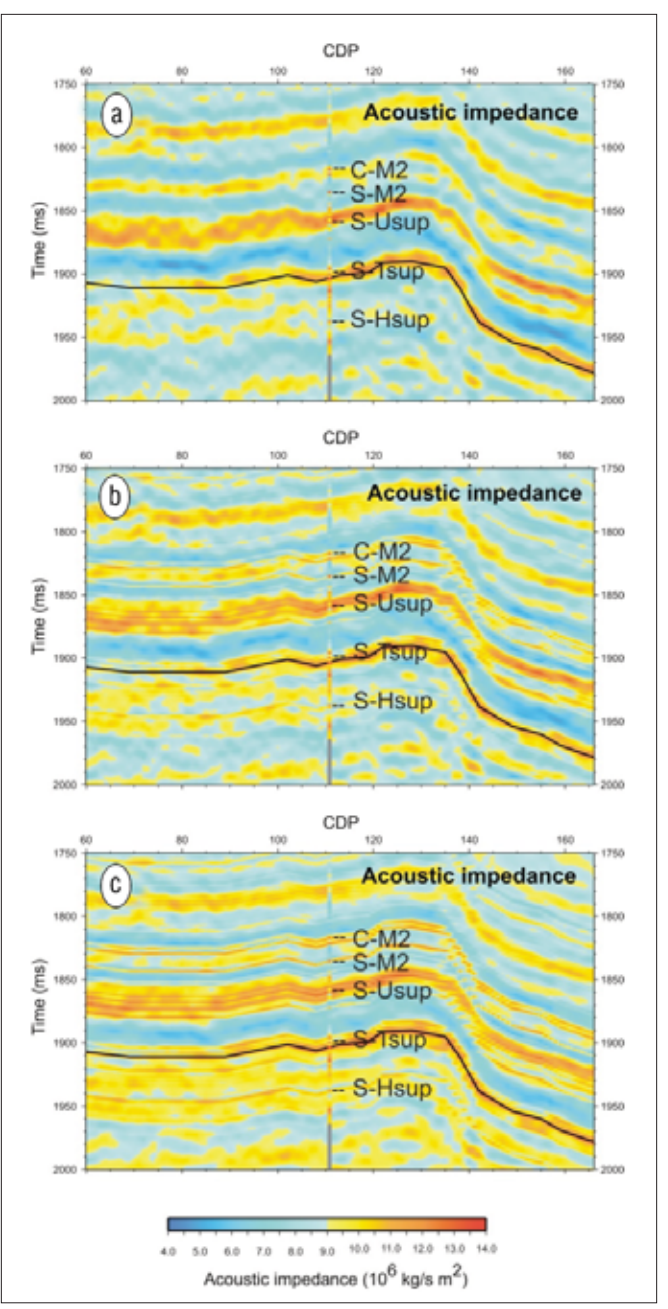


Figure 6. (a) Zoom of acoustic-impedance section with no well conditioning shown in Figure 5. Acoustic impedance sections estimated from the seismic petrophysical inversion conditioned to the well-log data, (b) with a correlation factor of 0.5 between well-log and model properties, and (c) with a correlation factor of 0.7. The well-log acoustic impedance is superposed at the well and plotted with the same color palette as the inversion. Major strata are identified as shown in Figure 3. The black line shows the polygon used to guide the lateral covariance of the model to the well data.

and the inner stratified structure of major layers is shown, beyond normal seismic resolution, in many places.

The inversion jointly estimates the total-porosity field conditioned to the corresponding well-log porosities. Figure 7a shows the total porosity for no well conditioning, as obtained in the previous section. Figures 7b and 7c show the result of the total-porosity fields obtained with 0.5 and 0.7

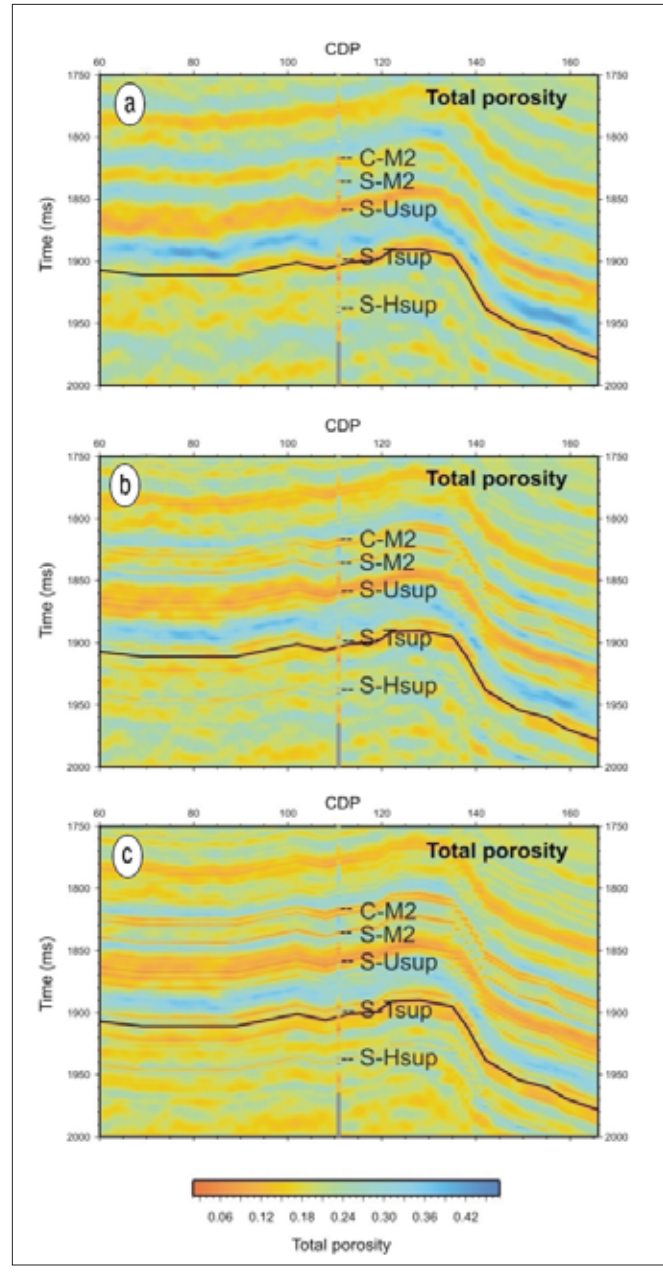


Figure 7. (a) Zoom on the total-porosity section estimated with no well conditioning shown in Figure 5. Total-porosity sections estimated from the seismic petrophysical inversion conditioned to the well-log data, (b) with a correlation factor of 0.5 between well-log and model properties, and (c) with a correlation factor of 0.7. The well-log-derived total porosity is superposed at the well and plotted with the same color palette as the inversion. Major strata are identified as shown in Figure 3. The black line shows the polygon used to guide the lateral covariance of the model to the well data.

maximum correlation across model and well-log properties. The estimated porosity fields for the geostatistical inversion show the same improved vertical resolution as the acoustic-impedance sections, indicating the thinner stratification. Vertical thin structure largely depends on the conditioned well-log data; there is also clear lateral heterogeneity for the total porosity and the acoustic impedance, shown, for instance, by discontinuous segments of the thin layers, which is influenced by the seismic information.

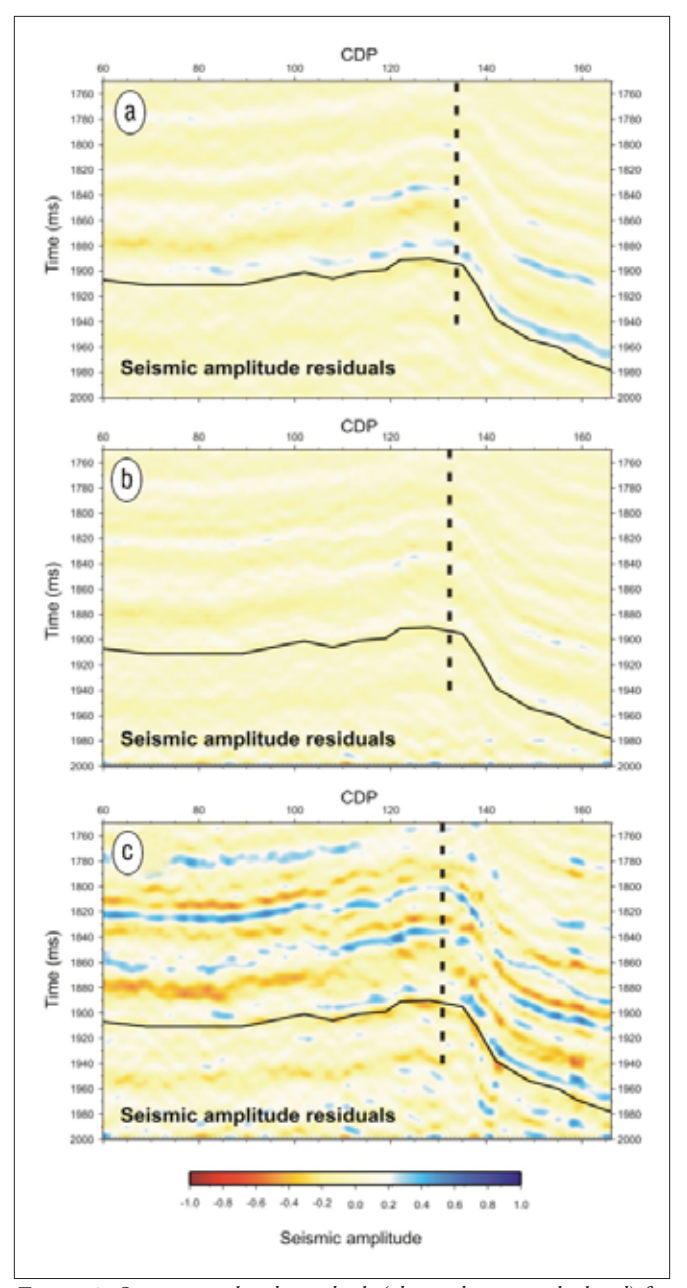


Figure 8. Seismic amplitude residuals (observed minus calculated) for the petrophysical seismic inversion with (a) no well conditioning, (b) conditioned to the well-log data with a maximum correlation factor of 0.5, and (c) conditioned to the well-log data with a maximum correlation factor of 0.7. The dashed line indicates the conditioning well, and the continuous line indicates the polygon used to guide the lateral covariance of the model to the well data.

The seismic data calculated from the estimated models using the geostatistical and petrophysical seismic inversion fit within data uncertainties (Figure 8). The figure shows the data residuals (observed minus calculated seismic amplitudes) for the unconditioned petrophysical inversion (Figure 8a), the well-log conditioned inversion with 0.5 maximum correlation (Figure 8b), and the well-log conditioned inversion with 0.7 maximum correlation. In these residual plots, the color scale is four times smaller than the corresponding one for total amplitudes in Figure 4. The 0.5 maximum correlation between the well-log and model properties produces an

optimal fit with the observed data. The seismic data fitting slightly degrades for the 0.7 maximum correlation, indicating that the model is, in this case, overconstrained to the well-log data.

### Discussion and conclusions

We have applied a seismic and petrophysical inversion method to estimate acoustic impedance and total porosity in an oil-producing area of Ecuador. The information provided by the inversion proved useful for the delineation of major strata: shale on one side, characterized by high porosity and low impedance; limestone and sandstone on the other side, characterized by lower porosities and higher impedances. The same analysis indicates that the fluid effect (oil brine) is beyond the resolution of the acoustic inversion in this case. More information could be obtained with an elastic formulation of the inverse problem using data at several offsets or incidence angles.

The petrophysical seismic inversion allowed us to jointly map the acoustic impedance and the total porosity fields, which showed good correlation with the corresponding impedance and porosity estimated directly from well logs. Their agreement is a good indication of the adequate results obtained with the petrophysical seismic inversion.

In a second step, we apply a geostatistical constraint to the petrophysical seismic inversion (assuming a positive correlation between well logs and seismic-derived property fields). The results of the geostatistical and petrophysical seismic in-

version show higher-resolution features away from the well path, imprinted from the well log's thinner vertical structure but also controlled by the lower-resolution information from seismic

Well-log-derived properties and medium properties are correlated. However, they should not be considered identical as well logs are subject to uncertainties. Adjusting a correlation factor across the model and well-log properties produces an optimal explanation of the seismic data and avoids overconstraining the model to the well-log data. On the other hand, inversion results adequately conditioned to the well-log data improve the seismic data fit in comparison with the inversion without well-log constraints.

**Suggested reading.** "The optimization approach to lithological inversion: Combining seismic data and petrophysics for porosity prediction" by Bosch (Geophysics, 2004). *Seismic Amplitude Interpretation* by Hilterman (SEG, 2001). "Petrophysical seismic inversion conditioned to well-log data: Methods and application to a gas reservoir" by Bosch et al. (Geophysics, 2009).

Acknowledgments: We thank Suelopetrol (Venezuela) and the Consorcio Petrolero Amazónico (Ecuador) for their interest in this work and the authorization to publish the results.

Corresponding author: miguel.bosch@cantv.net